ACS OMEGA

http://pubs.acs.org/journal/acsodf

Article

Transformation of Amphiphilic Antiviral Drugs into New Dimensional Nanovesicles Structures

Suzana Hamdan, Bapurao Surnar, Alexia L. Kafkoutsou, Luciano Magurno, Sapna K. Deo, Dushyantha T. Jayaweera, Shanta Dhar, and Sylvia Daunert*

Cite This: *ACS Omega* 2022, 7, 21359−21369

Read Online

ACCESS | Metrics & More | Article Recommendations | Supporting Information

ABSTRACT: Improved techniques were applied to formulate drugs into dimensional nanostructures, doped "nanovesicles". These nanovesicles are solely composed of self-assembled amphiphilic antiviral agents used for the treatment of viral infections caused by flaviviruses, such as Zika virus. Studies were done to evaluate the effectiveness of the syntheses, formation, and performance under different experimental conditions, and behavior of the drug nanovesicles *in vitro* and *in vivo*. These studies demonstrated that assembling the hydrophobic antiviral drug molecules into nanodrugs is a successful technique for the delivery of the therapeutic agents, otherwise difficult to be supplied. Our studies confirmed that this nanodrug preserved and, in many cases, enhanced the embedded cellular activity of the parental free drug molecules, both *in vitro* and *in vivo*. This proposed formulation is highly important as it addresses the issue of insolubility and low bioavailabiity of a wide range of highly potent pharmaceutical drugs—not limited to a specific class of antiviral drugs—that are of high demand for the treatment of medical conditions and emerging pathogens.

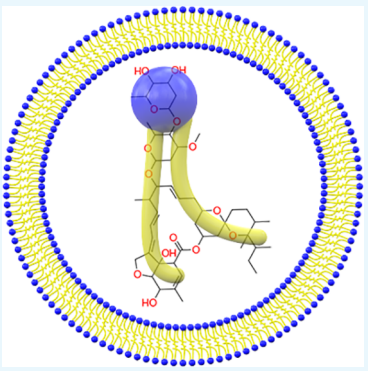

INTRODUCTION

We report in this work, for the first time, a versatile procedure to address the insolubility in aqueous medium of hydrophobic antiviral drugs and the urgent need to apply this drug for treatment of viral infection. We designed a new configuration of assembled drug molecules at the nanoscale, with the morphology of nanovesicles structures. In this case, the vesicles are composed solely of assembled amphiphilic drug molecules. The formation of this drug-based structure introduces a novel drug delivery method different from the norm,[1] wherein the nanovesicles present dual synergetic benefits:[2] transportation efficiency and therapeutic efficacy of the drug.[2] This combination should allow the delivery of an increased number of drug therapeutics without the need for carriers as the carrier is the drug itself, thus avoiding problems associated with low loading capacity and unknown metabolism of the carrier/vehicle in the body. Further, the nanovesicles can be efficiently applied in aqueous medium in the absence of any toxic organic solvent, which is highly significant for biological applications. The vesicles of interest are composed of antiviral drug molecules with amphiphilic structures and comprehensive hydrophobic property. The amphiphilic property controls the assembly mechanism of the drug molecules, contributing to vesicular structures. This new design is beneficial for different methods of drug delivery since it eliminates the need for the use of penetration enhancers such as surfactants,[3−7] usually added to the nanovesicles suspensions.

Nanovesicles are nanotechnology-based delivery systems that are nature-inspired by biological systems such as red blood cells, exosomes, and pathogens.[4−7] These intriguing structures are capable of transporting their contents across cellular membranes to deliver a specific message for the execution of a biological activity or function.[8] Further, nanovesicles possess unique flow properties depending on their shape,[9,10] which endows these structures with tunable cellular uptake.[10] In this context, nanovesicles have gained particular importance due to their ability to enhance permeation rates of cargos,[11] that is, drugs, through resistant biological membranes, mainly the skin barrier.[12] The vesicle/cargo nanoscale system contributes to a major improvement of several pharmacokinetic properties of the cargo, including and not limited to, solubility properties, controlled release rates, and milieu sensitivity (pH and type of medium). Thus, a number of biological applications benefited from the use of nanovesicles as diagnostic tools[13,14] and therapeutics carriers.[13−15] However, there is still a high need to design reliable methods for the fabrication of biomimetic nanovesicles.[16] The method of preparation presented in this article aims to develop drug-based vesicles armed with intrinsic therapeutic functionalities, enhance the solubility properties of the drug in biological fluids, and design the preferred

Received: October 14, 2021
Accepted: March 18, 2022
Published: June 14, 2022

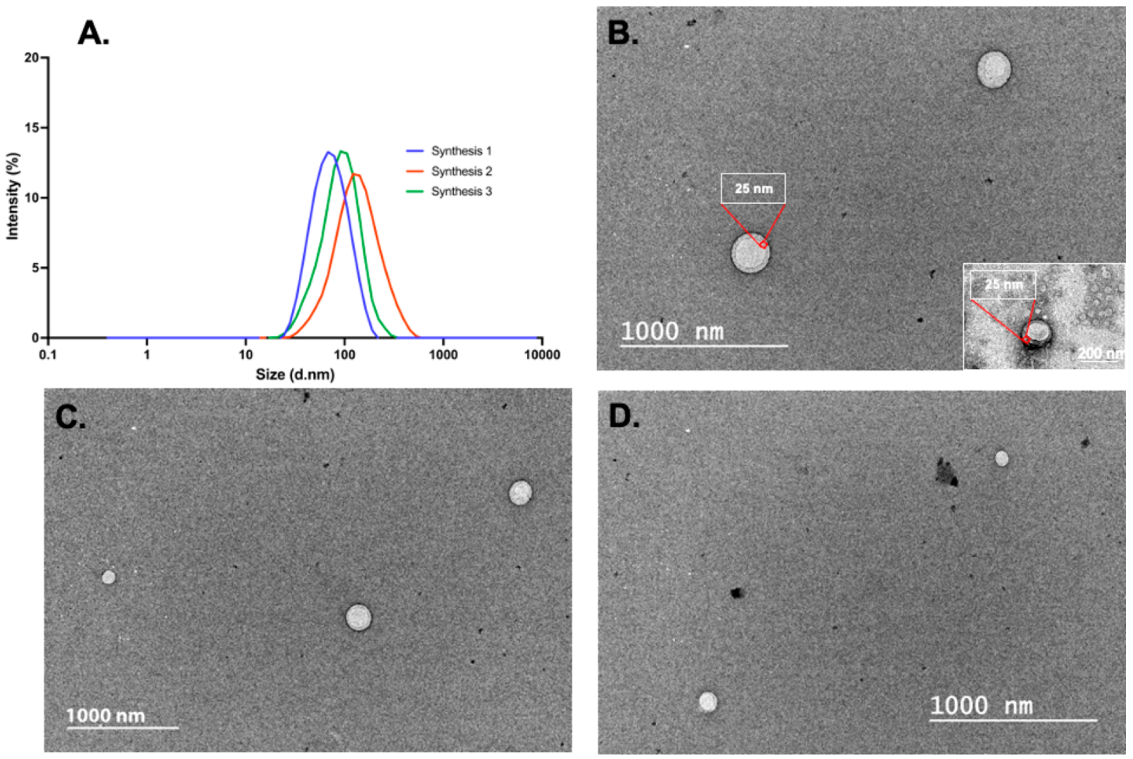

Figure 1. (A) Variation of hydrodynamic diameter of nano-IVM formulated in aqueous medium using ultrasound-assisted reprecipitation method (size of 103 nm, average of 12 replicate samples, 3 runs each, visualization of three replicate syntheses), and (B–D) TEM unstained micrographs of nano-IVM obtained using the same technique. Inset of panel B depicts 4% uranyl acetate stained micrograph.

configuration for optimal pharmacokinetic characteristics in drug delivery applications.

Herein, we have prepared nanovesicles derived from the drug ivermectin (IVM), which has reported efficient antiviral activity against flaviviruses,[17] such as Yellow Fever, Dengue, and Zika Viruses. IVM is listed as an FDA-approved drug candidate that decreased Zika Virus (ZIKV) infection in HuH-7 cells (EC_{50} between 1 to 10 μM) and other human cell lines.[18,19] It has been reported just recently as a potential drug for inhibiting the replication of SARS-CoV-2, which causes the coronavirus disease COVID-19.[20] For this recent study, IVM was tested on Vero-hSLAM cells 2 h postinfection and has shown ~5000-fold reduction in viral RNA at 48 h. However, the potent action of the drug ivermectin, as reported in the case of ZIKV, is only observed at high micromolar concentrations, which can result in severe toxic effects to cells. To address this issue, we hypothesized that a formulation of IVM molecules into nanostructures, that is, nano-IVM in our case, will increase absorption and, thus, lower the effective dose of IVM drug to be administered that is needed to combat the virus, avoiding toxicity and manifestation of side effects.[21] The formulation of self-assembled nano-IVM should aid in "solubilizing" IVM, a challenge for this drug that has been previously reported as an unstable drug in water.[22] This poor solubility in water is a common problem found with highly efficient hydrophobic drugs. IVM is, thus, an example of a drug that, once formulated at the nanoscale in physiological (aqueous-based) medium leads to an enhanced successful delivery to the target. To that end, herein, we report a versatile method for the preparation of nano-IVM vesicles; this synthetic method is applicable as well for a wide range of highly potent pharmaceutical drugs with poor water solubility, mainly targeting drugs within class II of the Biopharmaceutical Classification System (BCS) that suffer from a low bioavailability.[23] More specifically, the vesicular structure is related to pharmaceutics from this class that present both polar and nonpolar functional moieties, organized in a bilayer-like structure, due to molecular interactions (e.g., hydrophobic, hydrogen bonding).

RESULTS AND DISCUSSION

In our work, nano-IVM vesicles were prepared following an optimized reprecipitation method,[24] wherein the drug was dissolved in a good solvent (ethanol) at millimolar concentration, and its ethanolic solution was added (in small increments) to a poor solvent (water) to allow the precipitation of the nanovesicles. Ethanol was chosen in particular for its high miscibility in water, high vapor pressure, and as a good solvent for ivermectin drug. The synthesis was assisted with ultrasound (ultrasonication bath) for a better size-control of the nanomaterials, which was achieved by the action of acoustic cavitations to promote intermolecular interactions.[25] The nanovesicles were analyzed using materials characterization techniques and optical properties, in addition to the release studies at the physiological pH. Dynamic light scattering (DLS) and transmission electron microscopy (TEM) were initially used to estimate the size and morphology of the nanomaterials at neutral pH. DLS measurements of 12 syntheses revealed an average size of 103 nm (103 ± 31.9 nm, N = 12) for nano-IVM (hydrodynamic diameter) after 24 h from its synthesis (Figure 1A depiction of three representative replicate samples), whereas the TEM micrographs revealed nanodrugs of an average size of 95 nm (Figure 1C,D). For better visualization of the formation of the nanovesicles Figure 1B depicts a larger size of unstained nano-IVM while the inset

https://doi.org/10.1021/acsomega.1c05758
ACS Omega 2022, 7, 21359−21369

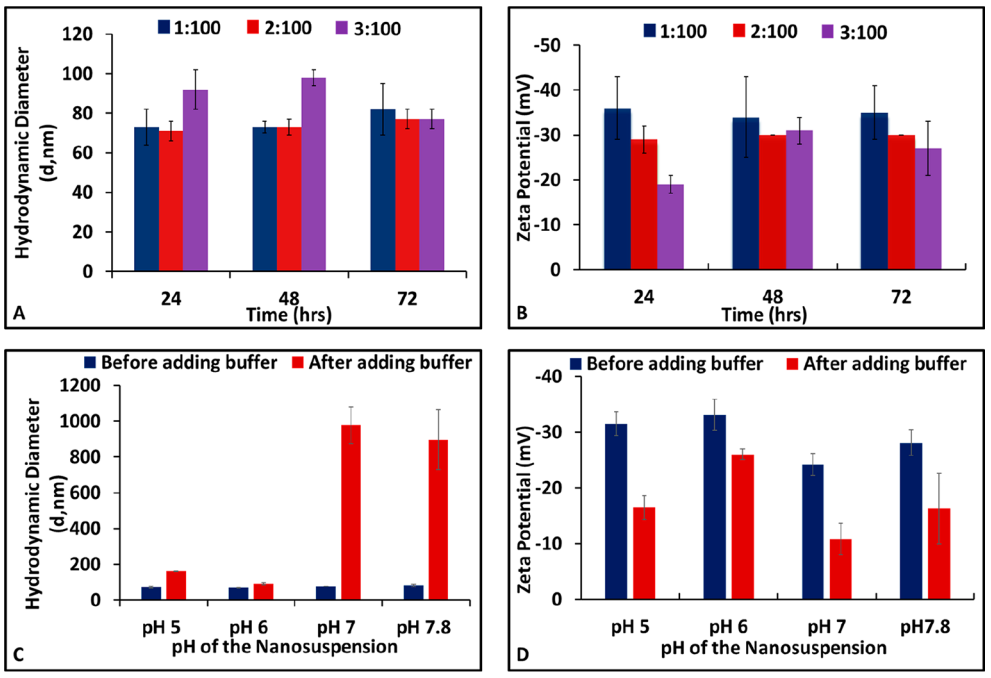

Figure 2. Change of (A) diameter and (B) zeta potential with volume ratios of ethanolic IVM solution (1 mM) to volume of water during the time growth of nanomaterials. Change of (C) diameter and (D) zeta potential with the pH of the suspension before and after the addition of a buffer.

shows a nanovesicle stained with 4% uranyl acetate. The thickness of the vesicular membrane was determined as 25 nm (Figure 1B inset). The self-assembly of IVM amphiphilic molecules into nanovesicles is demonstrated under aqueous conditions. This mechanism is governed in this case by hydrophobic and hydrogen-bonding interactions among the drug molecules and is able to overcome the undesirable hydrophobic water interactions. Our hypothesis is that the hydrophilic part of IVM acts as a head and the hydrophobic acts as a tail to form a vesicular structure. The amphiphilic nature of ivermectin was determined via calculation of the partition coefficient (log *P*) both experimentally and theoretically through the Chemdraw software. Our findings suggest that the hydroxy groups of IVM act as the head part of the amphiphilic moiety as they are more hydrophilic compared to the remaining structure. (Figure S1 in the Supporting Information). The zeta potential measurements were conducted to determine the electrostatic surface potential and evaluate the stability of the suspensions in aqueous medium (filtered water). The zeta potential (ζ) value was −27 mV (average zeta potential values of 12 replicate suspensions, 3 runs per synthesis) with pH of the medium being 7.4. The synthesized nanodrugs present an acceptable stability and exhibit minimal level of agglomeration considering that the zeta potential value is close to the limit value (−30 mV), globally accepted as the normal value reflecting the stability of suspensions.[26,27] The presence of this high surface charge contributes to an electrostatic repulsion among the vesicles and causes a decrease in the level of agglomeration. We monitored the concentration- and pH-variations versus time of nanovesicles aging to further understand the formation of vesicles-like aggregates (Figure 2). The data showed that the hydrodynamic diameter is similar for the 1:100 and 2:100 volume ratios of drug in ethanol to volume of water (Figure 2A); however, the volume of 3:100 resulted in a larger size of vesicles that was monitored during 24 and 48 h of growth time. The hydrodynamic diameter produced from the 3:100 volume ratio levels off with other volume ratios-based suspensions after 72 h. Nano-IVM structures might have redistributed and stabilized after a sufficient time of growth or aging. Zeta potential measurements studies were also performed on IVM suspensions prepared using different volumes of ethanolic solutions demonstrating that the changes in such composition has minimum effect on the stability of nano-IVM (Figure 2B). The evaluation of the surface charge of these nanovesicles reflects the optimal interaction of nanomaterials with the biological target, as well as the bioavailability of these materials. The pH stability of these suspensions was also evaluated by resuspending the aqueous suspension of nano-IVM in different pH buffers (Figure 2C,D). The effect of pH on the formulations in terms of size and stability demonstrated that the nanomaterials aggregated at pH 7.0 and 7.8, but remained stable at lower pH. This platform allows the administration of IVM through the oral route, as the nano-IVM remains stable at pH values similar to those of the gastrointestinal tract. The long-term storage of nano-IVM was also assessed after two months at 25 °C from their preparation in aqueous medium (filtered water), which is important for the potential use of this compound as a pharmaceutical product. The fabricated nanostructures revealed a long-shelf life (at least 2 months, (84 nm size)) and a high colloidal stability (−32 mV), an advantage that was observed in difference to what conventional liposomes present (Figure S2 in the Supporting Information). Thus, the hydrophobic interactions among IVM molecules are proven to be stronger than the interactions with water molecules. These formulations do not destabilize during the formation process and under the reported synthesis conditions, which endows them with a physicochemical stability, unlike typical lipid-based vesicles.[28−30]

The optical properties of nano-IVM were also evaluated, taking into consideration that these properties might be size-dependent as it is often observed in the case of organic

https://doi.org/10.1021/acsomega.1c05758
ACS Omega 2022, 7, 21359−21369

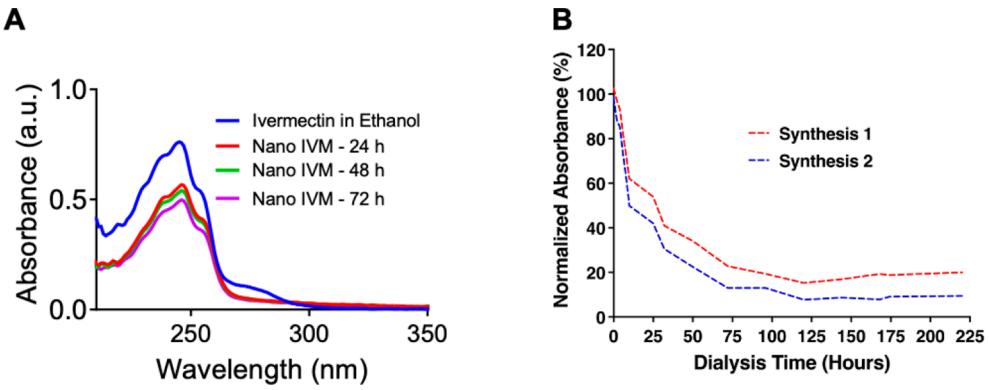

Figure 3. Optical properties of nano-IVM: (A) Absorbance spectra nano-IVM suspensions aged for 24, 48, and 72 h (final concentration of 20 μM in water), and of bulk IVM (20 μM in ethanol). (B) Release profile of nano-IVM vesicles in PBS buffer pH 7.4; plot of moving average of duplicate syntheses.

nanomaterials.[31] Nanomaterials usually exhibit optical properties that lie between atomic and bulk properties.[32] Their properties differ from their bulk counterpart as a result of the inter- and intramolecular interactions that contribute to the formation of the nanomaterials. It is important to understand the changes of optical properties for nano-IVM and the type of molecular arrangement that controlled the formation of nanovesicles. For this purpose, nano-IVM suspensions were synthesized under aqueous conditions using the modified reprecipitation method, then left to age for 24, 48, and 72 h (Figure 3A). The bulk of IVM was prepared following a similar procedure in ethanol, and both bulk and nano-IVM were compared at the same concentration. The properties of the nanosuspensions were similar indicating consistency in the preparation method (same average size of 80 nm) and stability of the suspensions over time. The conjugated-diene chromophore of ivermectin has an ultraviolet absorbance maximum at 245 nm.[33] Both solutions and suspensions were consistent in terms of optical properties, with absorbance ranging between 230 and 260 nm. However, the nano-IVM suspensions showed a decrease in the molar absorptivity in comparison to the bulk material, as a result of the presence of intermolecular electronic interactions upon aggregation. The decrease of the cross-section of nano-IVM exposed to the light can also contribute to the decrease in absorbance value. Our previous studies have shown size stability of nano-IVM suspensions (for 2:100 volume ratio) at various aging periods (or growth time) (Figure 2A,B).

A continuous dialysis of the nanovesicles suspensions in a phosphate-buffered saline PBS solution (pH 7.4) was also performed to evaluate the release profile, more precisely the degradation profile of the nanovesicles (Figure 3B). The suspensions were prepared in duplicate using the optimized reprecipitation method, with a ratio of 2:100 of 1 mM ivermectin drug. After 24 h, the nanomaterials were suspended in PBS and dialyzed against PBS buffer pH 7.4. Nano-ivermectin showed first a burst release of 20% of its molecules or entities, suggesting that those molecules were not strongly bound to the assembled nanoscale aggregates, and were a possible source of vesicles agglomeration. The nanovesicles kept then a slower and sustainable release for a long period of time, about 220 h. Overall, the general profile of the release/degradation rate implies a maintained efficacy of nano-ivermectin for several days. This behavior is advantageous because it reflects a controlled release of the therapeutic agents under physiological conditions. Thus, the activity of the antiviral agents can be modulated and become more effective for the pharmacological effect, in this case, inhibition of the viral replication.

To better evaluate the efficiency of preparing nanodrugs (nanovesicles form antiviral drug) in terms of successful delivery of the therapeutic molecules, we decided to develop an experimental test that can assist us in evaluating the importance of this nanoscale design for biological applications. For this purpose, different volume ratios of ethanolic ivermectin to water were used during the syntheses. Volume ratios of ethanolic IVM to water 0.5:100, 1:100, 2:100, 3:100, 4:100 were explored. These ratios correspond to different concentrations of nanomaterials (nano-IVM): 5, 10, 20, 30, 40 μM, noting that for the 0.5:100 volume ratio (5 μM), nano-IVM will not form because the concentration of ivermectin molecules is not sufficient for the formation of stable assembly (below the solubility limit of IVM in water, 0.005 mg/mL[22]).

As comparison, similar concentrations of the free ivermectin molecules in water were also prepared: 5, 10, 20, 30, and 40 μM. The photos of the aliquots from each type of preparation prove that nano-IVM tends to be suspended in water (even after 72 h and at high concentration) versus ivermectin in water that sediments due to the insolubility of the drug in water, especially at high concentrations (10, 20, 30, and 40 μM) (Figure 4 in manuscript and Figure S3 and S4 in Supporting Information). These observations detail that the technique of transformation of free drug molecules into nanodrugs improves the "solubility" of the therapeutic molecules, allowing the delivery of the drug even at high concentrations without the aid of an excipient or a solubilizing agent, that is quite often needed for delivery purposes.

Further work has been performed to showcase that the conversion of single IVM molecules into nanovesicles does not negatively impact the *in vitro* activity of the drug. Therefore, cellular uptake of nano-IVM was tested using two different cell lines, Caco-2 and HEK 293T cells. Nano-IVM was uptaken by both cells: to a similar extent as its bulk counterpart for HEK 293T cells, but higher uptake level of nano-IVM by Caco-2 cells, about 10% increase in comparison to the bulk (Figure 5A,B). The mechanism of uptake at the nanocell interface for the nanoscale materials might be different than that for single molecules and needs further exploration. These data demonstrated the ability of the drug-based nanovesicles to successfully penetrate the cells, which makes these vesicular

https://doi.org/10.1021/acsomega.1c05758
ACS Omega 2022, 7, 21359−21369

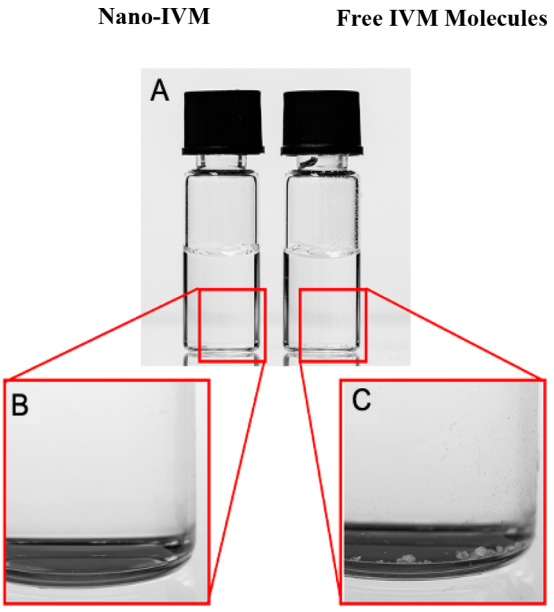

Figure 4. (A) Comparison of nanodrugs (left) to free drugs in water (right) at 40 μM; (B) solubilization of drugs and absence of drug particles at the bottom of the vial; and (C) presence of ivermectin at the bottom of the vial (insolubility, 56.5% free IVM dropped out).

entities to be highly effective as therapeutic agents, as the entry to the cells is an important step to achieve the desired prognosis. Another important parameter for the newly engineered nanomaterials is to understand their effect on cellular respiration (detailed seahorse experiments are reported in Supporting Information). More particularly, this study is essential for drug-based nanoscale materials, for it is important to evaluate their specific interaction with the cellular powerhouse, mitochondrion. Measurement of oxygen consumption rate (OCR) values in Caco-2 and HEK 293T cells indicated that IVM and nano-IVM both have an effect, to a different extent depending on the cell type, on OCR values and other parameters including basal respiration, maximal respiration, and ATP production; this effect was similar to IVM free molecules (Figure 5C,D). The observed change in energy metabolism is linked to the exposure time of cells to nanomaterials (after 24 h). IVM, as well as nano-IVM, caused a decrease in the maximal respiration in Caco-2 cells (Figure S5 in the Supporting Information); the effect was more pronounced in the case of HEK 293T cells where all the respiratory activities were significantly affected. This metabolism change is due to the structure of the IVM drug that is highly rich in electrophilic functional groups, causing an alteration in electron pathways of the mitochondrial respiratory chain. The aforementioned *in vitro* results are essential to portray the internalization of nanovesicles and their interaction with cell components, a process that is essential for biological

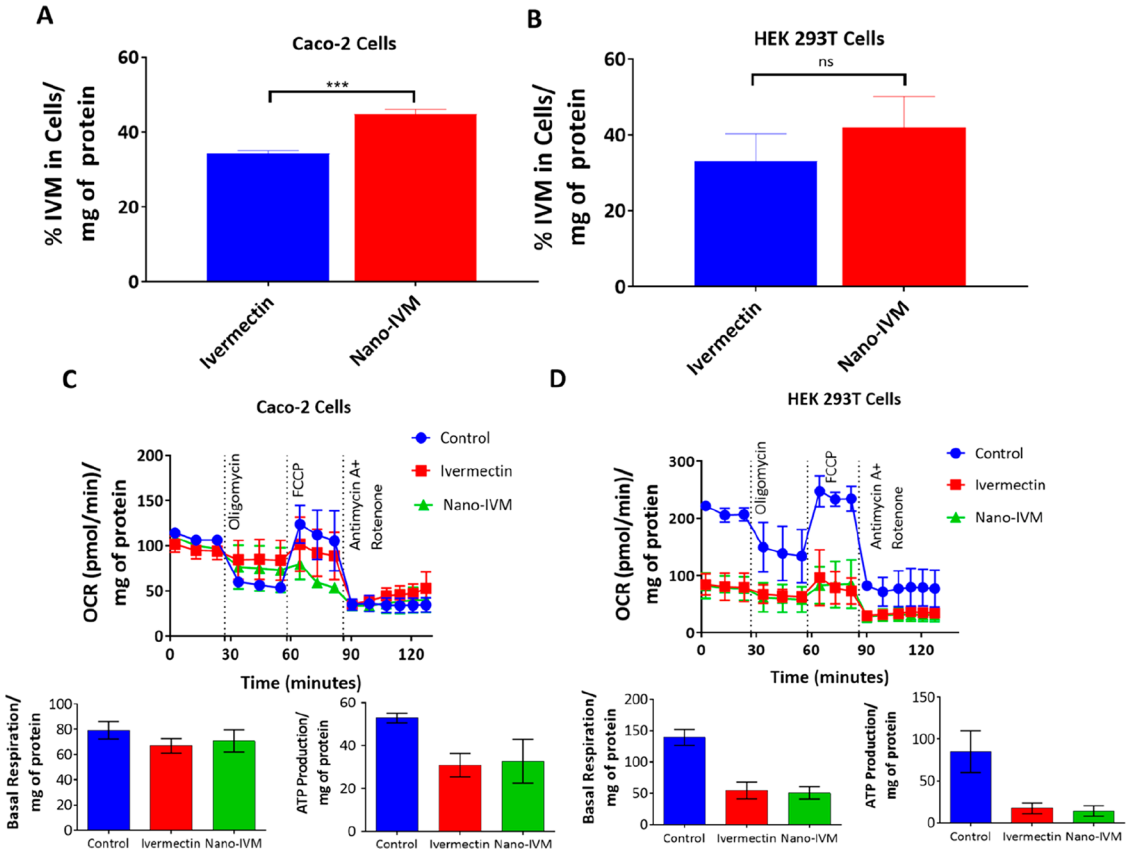

Figure 5. Cell uptake of nano-IVM in (A) Caco-2 and (B) HEK 293T cells. Cells were treated with IVM or nano-IVM at a concentration of 2 μM with respect to IVM, for 24 h. Analyses of mitochondrial respiration in (C) Caco-2 cells and (D) HEK 293T cells were done using Seahorse analyzer. Notation: oligomycin, ATP synthase inhibitor; FCCP, an uncoupling agent; antimycin A, a mitochondrial complex III inhibitor; rotenone, a mitochondrial complex I inhibitor. Cellular uptake data was analyzed using unpaired *t* test; *p*-value is less than 0.001 for (***); "ns" is for nonsignificant.

https://doi.org/10.1021/acsomega.1c05758
ACS Omega 2022, 7, 21359−21369

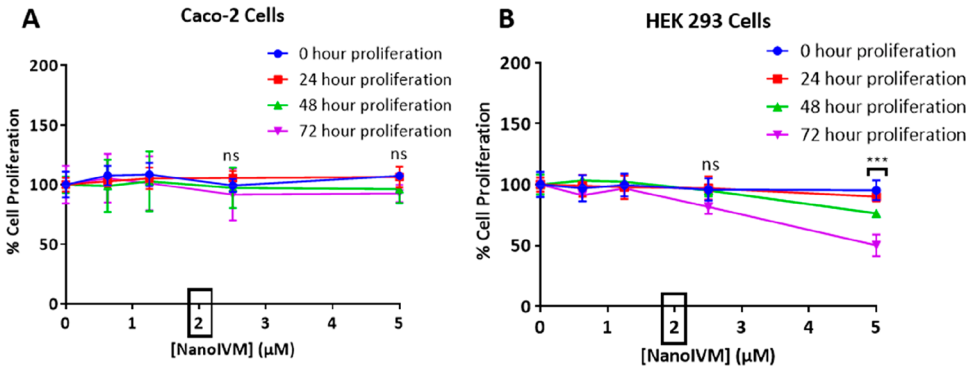

Figure 6. Cytotoxicity evaluation of nano-IVM using MTS proliferation assay with (A) Caco-2 cells and (B) HEK 293T cells. The nanovesicles did not show any toxicity at 2 μM concentration, which is the concentration investigated. Caco-2 cells were proliferating overtime with no toxicity even at the highest concentration (5 μM). HEK 293T cells showed toxicity at 5 μM only after 48 and 72 h of incubation with nano-IVM. Statistics were done using one-way anova (multiple comparisons), p-value is less than 0.001 for (***); "ns" is for nonsignificant. The highest significance was reported for a comparison between 0 and 72 h for HEK 293 cells at 5 μM.

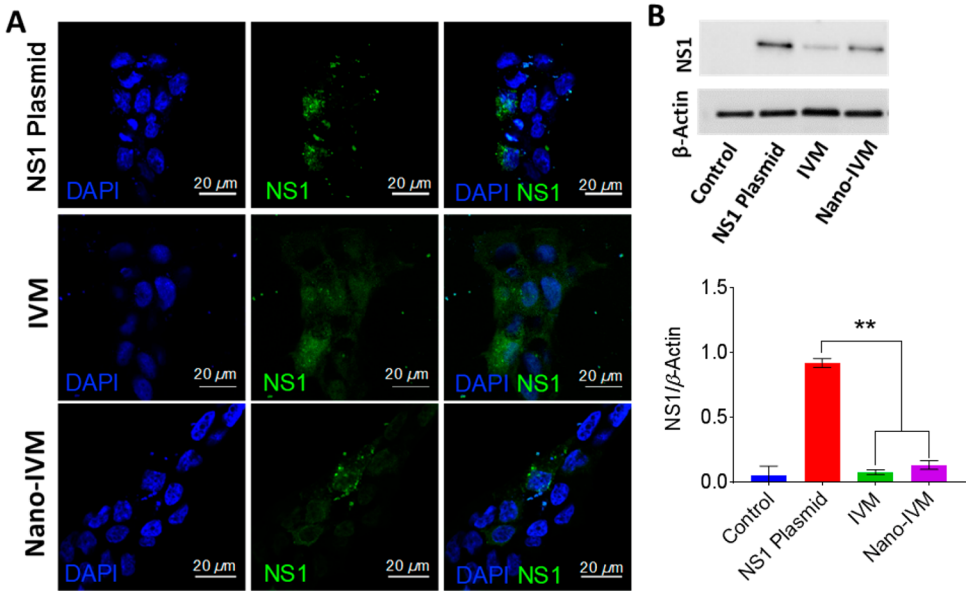

Figure 7. (A) Immunostaining for NS1 expression in HEK 293T cells. (B) Western blot for NS1 expression in HEK 293T (p = 0.0018). Cells were treated with IVM or nano-IVM at a concentration of 2 μM with respect to IVM for 24 h. The bars on the plot represent an average NS1 expression from duplicate of Western blots. The Y axis of the plot represents the expression level of NS1 normalized to ß-Actin, developed using chemiluminescence.

studies. It is also worth mentioning that nano-IVM is purely derived from the ivermectin drug; therefore, it is highly expected for these nanodrugs to exhibit a similar action on cells as the parental drugs, especially that these nanovesicles are delivering the utmost yield of the drug molecules, distinctively at the nanoscale level.

While the stress action of IVM and nano-IVM on the mitochondria, especially in the case of HEK 293T cell line, was showcased; it was important to raise the question about the cytotoxicity of the formulated materials (nano-IVM) especially at the investigated concentration (2 μM). Therefore, MTS proliferation assays were performed on Caco-2 and HEK 293 cells over the course of 72 h, and at various concentrations of nano-IVM (Figure 6A,B). Nano-IVM did not show any cytotoxic effect on Caco-2 cells; however, the cytotoxicity trends for HEK 293 cells were consistent with seahorse experiments where this type of cell line has shown more sensitivity toward nano-IVM drugs, albeit only at higher concentrations and for the longest exposure time. This observation is likely due to the difference in the membrane composition of the cells and the interaction mechanisms of nanodrugs with the cell membrane. Further studies indicate as well that Caco-2 cells were not extensively vulnerable toward nano-IVM in particular at extremely high concentrations where only 20% decrease of cells proliferation was measured after 72 h of nanodrugs incubation (MTS proliferation assays were done as high as 100 μM of nano-IVM, Figure S6 in Supporting Information). One aspect to consider in this assay is the hydrophobicity and surface properties of the system, especially that these physicochemical properties have been established to correlate with the level of the nano-IVM toxic effect on Caco-2 cells.[34,35]

In this context, we also performed specific studies to assess the antiviral activity of the formulated nano-IVM against Zika virus nonstructural 1 (NS1) protein (Figure 7). Both immunostaining and Western blot studies confirmed the

https://doi.org/10.1021/acsomega.1c05758
ACS Omega 2022, 7, 21359−21369

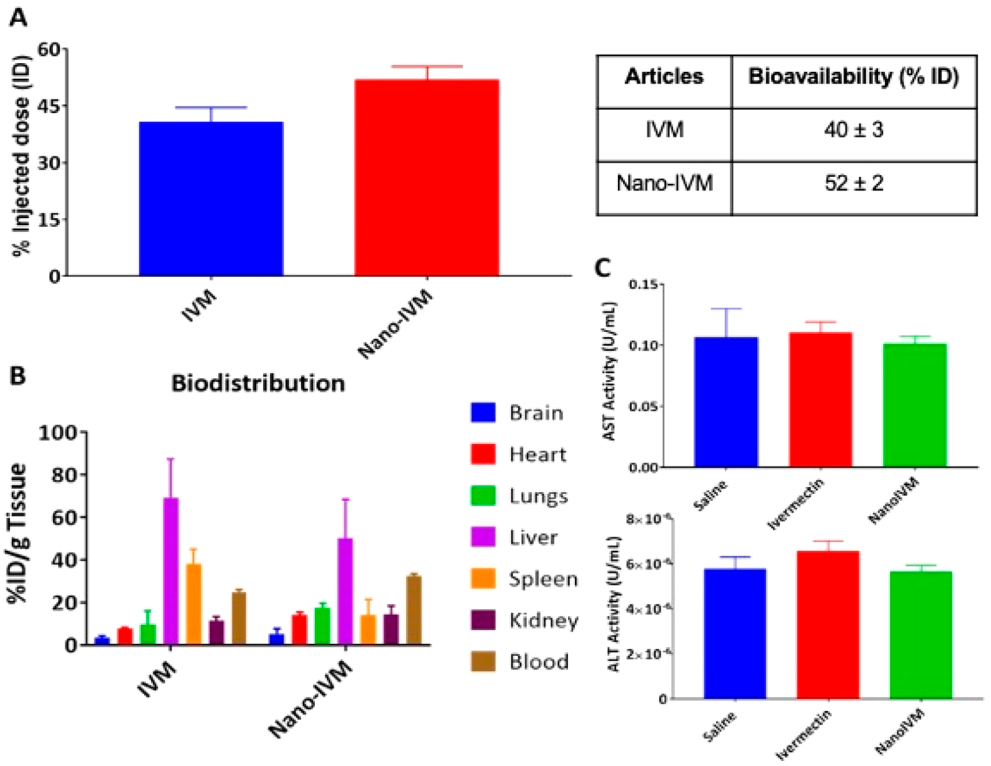

Figure 8. (A) Bioavailability of IVM and nano-IVM in Balb/c female mice after 24 h of administration by intravenous injection at a dose of 20 mg/kg with respect to IVM. The nano-IVM (assemblies of IVM drug molecules) showed approximately 10% increase in bioavailability after 24 h of injection (20 mpk), (B) Biodistribution of IVM and nano-IVM in different organs after 24 h of intravenous injection, and (C) AST and ALT levels in blood plasma of Balb/c female mice after 24 h of administration by tail intravenous injection at a dose of 20 mg/kg with respect to IVM. (n = 2 mice per group).

action of nano-IVM (as well as IVM) against the expression of NS1 protein, which is a glycoprotein that is involved in viral RNA replication and immune system invasion.[36] The NS1 protein expression in HEK 293T cells significantly decreased after IVM and nano-IVM treatment (Figure 7A) in comparison to the untreated cells. The results suggest that the designed antiviral nanovesicles still comprise the activity of their single antiviral molecules counterpart and can be active against ZIKV.

We further investigated the behavior of nano-IVM *in vivo*, to evaluate the bioavailability of the generated nano-IVM nanovesicles (Figure 8A). According to literature, the bioavailability of poorly water-soluble drugs, hydrophobic compounds, (regardless of the method of administration, and the mechanisms involved) is accounted as a significant challenge in the pharmaceutical industry.[37,38] Therefore, the concept of nanodrugs is expected to circumvent the issue of failing of drug delivery system and drug metabolism as a result of solubility- and mechanism-limited bioavailability. We anticipated an improvement in circulation times for nanodrugs as these nanomaterials can easily pass through fine blood cells and lymphatic endothelium,[39] as well as capillary permeability especially for nano-IVM vesicles. As observed, nano-IVM has shown a moderate improvement of the bioavailability in comparison to IVM; the results were recorded on a single time frame after 24 h of intravenous injection. Moreover, the most important detail to highlight in our case, when it comes to *in vivo* studies, is the improvement of nano-IVM delivery in comparison to IVM as a result of the increase of aqueous solubility of the nanosuspensions: nano-IVM was easily suspended in aqueous medium for delivery of the drug. Plus, IVM had to be dissolved in DMSO to facilitate the process, which adds toxicity to the formulation of an already toxic drug. The nanoformulation strategy applied to the preparation of nano-IVM demonstrates the easiness of its suspension and intravenous delivery, and solves issues related to the transport and delivery of therapeutic hydrophobic drugs.

Additionally, we performed animal studies and analyzed the biodistribution of both IVM and nano-IVM (Figure 8B) in mice. After 24 h of intravenous injection, both the IVM and nano-IVM-dosed mice showed more than 25% of injected dose (% ID) in blood: 25% for IVM and 32% for nano-IVM. It was noted that nano-IVM was less accumulated in the reticuloendothelial system (RES), liver, and spleen, (%ID/g tissue). This behavior of nano-IVM is comparable to that of sterically stabilized liposomes that have shown decrease of uptake by the RES system.[40] We can also speculate that the clearance mechanism of IVM is different than nano-IVM as a result of change of surface area, size, hydrophobicity property, solubility, and other physicochemical properties of the nanovesicles. Another observation in our case is the presence of nano-IVM in the lungs, especially delivered via intravenous injection, which is a good indication about the significance of this novel synthetic procedure of nanodrug that can be applied for treatment of respiratory diseases such as COVID-19. The nano-IVM showed in general a different distribution profile compared to free IVM in several organs including the lungs. Many factors related to the physicochemical properties of nano-IVM play a role in tissue penetration and distribution of nanovesicles in comparison to free molecules, in this case mainly the size, shape, charge, as well as the unique mechanical properties of nanovesicles that are associated with the mechanism of penetration across biological barriers.[41−43]

https://doi.org/10.1021/acsomega.1c05758
ACS Omega 2022, 7, 21359−21369

While these *in vivo* studies show promising results in terms of delivering nano-IVM to the biological system and preserving their internal efficiency, further studies are needed (larger number of mice) to statistically analyze the change of drug behavior as nanovesicles. Moreover, we studied the hepatotoxicity using ALT and AST activity assays. The ALT and AST levels were recorded in comparison to the control and no significant changes were detected, preliminary indicating the absence of hepatotoxicity and any negative effect of IVM or nano-IVM on the liver (Figure 8C). Further investigation is still needed to understand the metabolism of nano IVM *in vivo* including a more detailed hepatic panel; ultimately, what is definite from our previous experiments is the improvement of the delivery of the antiviral drug ivermectin that is claimed to be effective against flaviviruses and recently COVID-19, but challenging in terms of its solubility, transport, and biological behavior.

CONCLUSION

This work demonstrates the ability to generate nanovesicles that are assemblies of antiviral and amphiphilic drugs. This design presents a potential solution to deliver hydrophobic therapeutic agents, under physiological conditions and across resistant biological membranes, for treatment of viral infection, as well as other therapies that would benefit from the delivery of drugs formulated in the nanoscale. The proposed design does not require a carrier, thus avoiding possible side effects and loading problems. Further, this drug-based vesicles structure is superior to currently available forms of drug delivery that are prepared by using complex synthetic and optimization procedures. Herein, the nanosyntheses are based on the model antiviral drug IVM, that has shown effective properties against flaviviruses, but still suffers challenges in terms of its successful delivery as a nanoscale system. Our work combines efficiency, safety, and novel delivery method into one system that is needed for current advances in the biomedical field. In this work, nano-IVM was successfully synthesized as nanovesicles through a controlled technique based on a simple and direct ultrasonication-based reprecipitation method. The formation of the nanovesicles produced through assembly of IVM into nano-IVM, has shown increased solubility of the nanodrugs as a result of the downsizing of the drug into nanoscale. Furthermore, nano-IVM was promising in terms of its *in vitro* antiviral activity that was inherited from its parental single drug molecules, and presented, as well, promising bioavailability, biodistribution, and safety. The effective physicochemical and biological properties of nano-IVM are attributed to its unique formulation solely from drug molecules at the nanoscale, generating a potent drug delivery system for water-insoluble antiviral therapeutics. We envision that the proposed synthetic methods will be widely applicable in the nanoscale preparation of many other challenging hydrophobic drugs, including other antiviral drugs, and that this proposed method will find other applications in the fields of biomedical nanotechnology and nanomedicine.

EXPERIMENTAL SECTION

Materials. Ivermectin (Sigma-Aldrich, St. Louis, MO; R&D System Tocris, Minneapolis, MN), ethanol (Sigma-Aldrich, St. Louis, MO), sodium acetate trihydrate (J.T. Baker, Radnor, PA), sodium phosphate monobasic monohydrate (Sigma-Aldrich, St. Louis, MO), sodium phosphate dibasic (Sigma-Aldrich, St. Louis, MO), glacial acetic acid (BDH Chemicals VWR, Radnor, PA), sodium acetate anhydrous (Mallinckrodt Chemicals, St. Louis, MO), and uranyl acetate (Electron Microscopy Sciences, Hatfield, PA) were purchased and used as received. Phosphate buffered saline (1X PBS) was purchased from Gibco (Thermo Fisher Scientific, Waltham, MA). CellTiter 96 AQueous One Solution Cell Proliferation Assay (MTS) was purchased from Promega (Madison, WI) and used as directed. Alexa Fluor 488 goat antirabbit IgG secondary antibody was procured from Invitrogen (Thermo Fisher Scientific, Waltham, MA). Goat serum was obtained from Sigma-Aldrich (St. Louis, MO). Glutamine, penicillin/streptomycin, trypsin-EDTA solution, HEPES buffer (1 M in water), and sodium pyruvate were procured from Sigma Life Science (Sigma-Aldrich, St. Louis, MO). Dulbecco's Modified Eagle's medium (DMEM) and fetal bovine serum (FBS) were purchased from Gibco Life Technologies (Thermo Fisher Scientific, Waltham, MA). Zika virus NS1 antibody (EA88) was purchased from Invitrogen (Thermo Fisher Scientific, Waltham, MA). Flag-tagged Zika NS1 plasmid was procured from Addgene (Watertown, MA). Ammonium persulfate, tris/glycine/SDS buffer, SDS-PAGE gel preparation kit TGX stain-free, fast cast acrylamine 10% and Clarity western ECL substrate were purchased from Bio-Rad Inc. (Hercules, CA), nitrocellulose membrane, and tween-20 was purchased from Fisher Bioreagents (Thermo Fisher Scientific, Waltham, MA).

Animals. Balb/c albino male and female mice (8 weeks old) were purchased from Jackson Laboratory. All animals were handled in accordance with "The Guide for the Care and Use of Laboratory Animals" of American Association for Accreditation of Laboratory Animal Care (AAALAC), Animal Welfare Act (AWA), and other applicable federal and state guidelines. All animal work presented here was approved by Institutional Animal Care and Use Committee (IACUC) of University of Miami (UM) Miller School of Medicine. All housing, surgical procedures, and experimental protocols were approved by the IACUC Committee of UM. Animals had free access to chow diet and water during all experiments.

Instrumentation. Instruments used included the Zeta-sizer Nanoseries (Nano ZS90, Malvern, UK), JEM-1400 TEM instrument (JEOL, München, Germany), carbon-coated 400-mesh TEM grids (Ted Pella, Redding, CA), NanoDrop spectrophotometer (Thermo Scientific, Waltham, MA), DeNovix spectrophotometer/fluorometer (Wilmington, DE), Float-A-Lyzer G2, MWCO: 3.5−5 kDa (Spectrum Laboratories, Irving, TX), Elga model PURELAB flex water filtration system (United Kingdom), and Branson 200 ultrasonic cleaner (Branson, Danbury, CT). Distilled water was purified by passage through a Millipore Milli-Q Biocel (Woburn, MA) water purification system (18.2 MΩ cm) containing a 0.22 μm filter. Absorbance analyses were performed on a Bio-Tek Synergy HT and BMG Labtech Clariostar microplate readers. Strata C18-T columns (catalog number 8B−S004-EAK) were purchased from Phenomenex. High-performance liquid chromatography (HPLC) analyses were made on an Agilent 1200 series instrument equipped with a multiwavelength UV−visible and a fluorescence detector. Cells were counted using Countess automated cell counter procured from Invitrogen and Moxi Z automated cell counter from ORFLO Technologies. Mitochondrial bioenergetics assays were performed on XFe96 Extracellular Flux Analyzer (Agilent Seahorse Biosciences, Santa Clara, CA). Western blots were imaged using ChemiDoc imaging system (BioRad). Confocal

https://doi.org/10.1021/acsomega.1c05758
ACS Omega 2022, 7, 21359−21369

microscopy images were obtained using an Olympus FluoView FV3000 (Center Valley, PA).

METHODS

Preparation of Nano-ivermectin (Nano-IVM). A volume (50−150 μL) of ethanolic ivermectin (1 mM) was added to a volume of 5 mL of filtered water, under bath sonication for 5 min. Ultrapure water (18.2 MΩ cm) was filtered using a 0.45 μm syringe filter. The sample was left, covered with punctured parafilm, to age for 24 to 72 h. The suspension was sonicated before any measurement.

pH Effect. A volume of 900 μL of ivermectin nanosuspension was added to 100 μL of 0.1 M of the buffer (different pH values). The mixture was sonicated for few minutes before measurement.

Optical Properties. The syntheses of nano-IVM suspensions (2:100 volume ratio of ethanol to water) were performed on different days to let the suspensions age for different periods (24, 48, or 72 h). All the nano-IVM suspensions were prepared in duplicate (two suspensions/day for each aging time). The bulk (ivermectin solution in ethanol) was prepared on the same day using equal concentrations of nano-IVM suspension. The nanosuspension is usually covered with punctured parafilm, while the bulk solution is capped. The controls were prepared as well. The first control is a mixture of ethanol/water for nano-IVM suspension (2:100 volume ratio of ethanol to water); the second control is ethanol for bulk ivermectin.

"Solubility" Assay. Nano-IVM suspensions were prepared using the modified reprecipitation technique presented earlier (Preparation of Nano-ivermectin). In this assay, different volumes (25−200 μL) of 1 mM ethanolic ivermectin were used. The syntheses were done in 5 mL volume of water. These preparations were left to age for 24 h before taking aliquots for imaging. To compare the preparations to ivermectin solutions, the corresponding concentrations were used, and 5−40 μM concentrations of ivermectin drug were prepared in water and then put on the shaker overnight for an attempt to dissolve the drug in water. Photos were taken following the preparation of ivermectin and nano-ivermectin. Phase contrast images were also taken to confirm the absence or presence of sedimentation. The calculation of free drug precipitation was performed by collection of the precipitate and measurement on a high sensitivity scale.

Dialysis Studies. Two nano-IVM suspensions were prepared. After 24 h, a volume of 4.5 mL of each suspension was added to 0.5 mL of 100 mM PBS buffer 10×. The mixtures were sonicated and added to the dialysis tube. The dialysis was against a volume of 500 mL of 10 mM PBS buffer 1X. The dialysis was performed under magnetic stirring. Aliquots from the dialyzate were used for absorbance measurements, and then returned to the original suspension. The measurements were initially performed after 2 h, then after 24 h for almost 9 days when the absorbance value stabilized. The dialysis medium was frequently replaced with a fresh PBS buffer during the dialysis.

Cell Culture Methods. Human epithelial colorectal adenocarcinoma (Caco-2) cells were procured from ATCC (Manassas, VA). These cells were grown in Dulbecco's Minimum Essential Medium (DMEM) along with 20% of fetal bovine serum. A transfectable derivative of human embryonic kidney 293 (HEK293T) cells were also procured from ATCC (Manassas, VA). These cells were grown in Dulbecco's Minimum Essential Medium (DMEM) along with 10% fetal bovine serum. Cell cultures were maintained in a humidified cell culture incubator at 37 °C and with 5% CO_2.

Cellular Uptake. Caco-2 and HEK-293T cells were plated separately in a 6-well plate with a density of 50 000 cells/well in 2 mL of DMEM media. After 24 h, 2 μM of IVM and nano-IVM were added, and cells were incubated for 6 h. Cells were washed with PBS (3 times) and then collected in 1.5 mL centrifuge tubes and dissolved in 2 mL of acetonitrile. This mixture was sonicated for 20 min followed by centrifugation at 5000 rpm for 10 min. From the precipitated debris, the supernatant was gently collected. The ivermectin in supernatant was quantified using HPLC (wavelength = 243 nm at 21.01 min).

MTS Proliferation Assay. Several suspensions of nano-IVM were synthesized using a volume of 100 μL of 1 mM ethanolic ivermectin in 5 mL volume of water (see section Preparation of Nano-ivermectin). The suspensions were aged for 24 h. For high concentration studies, the suspensions were lyophilized to collect the dried nanomaterials at a high yield. For MTS proliferation assays, the nano-IVM were resuspended and sonicated in water, in order to have a 100 μM concentration of nano-IVM suspension. Several dilutions of nano-IVM were then prepared in water. In this assay, Caco-2 and HEK 293T cells were plated separately in a 96-well plate in DMEM at a confluency around 10^4 cells/mL, 200 μL per well. The cells were incubated at 37 °C, 5% CO_2 overnight. Different concentrations of nano-IVM and IVM were added to the cells and left for 72 h (0, 24, 48 h were tested as well). The MTS dye was added at that time frame before absorbance measurements. The dye was incubated for at least 30 min and the absorbance was recorded at 490 nm using a Clariostar microplate reader (BMG labtech, Cary, NC).

ASSOCIATED CONTENT

Supporting Information

The Supporting Information is available free of charge at https://pubs.acs.org/doi/10.1021/acsomega.1c05758.

Additional experimental procedures including storage stability study, solubility assay, mitostress assay, and MTS proliferation assay, and the methodology description of NS1 expression, biodistribution of nano-IVM, aspartate aminotransferase activity, and alanine aminotransferase activity (PDF)

AUTHOR INFORMATION

Corresponding Author

Sylvia Daunert − *Department of Biochemistry and Molecular Biology, University of Miami School of Medicine, Miami, Florida 33136, United States; Dr. JT Macdonald Foundation Biomedical Nanotechnology Institute of the University of Miami, Miami, Florida 33136, United States; Sylvester Comprehensive Cancer Center, Miami, Florida 33136, United States; University of Miami Clinical and Translational Science Institute, Miami, Florida 33136, United States;* orcid.org/0000-0003-4760-5528; Email: SDaunert@med.miami.edu

Authors

Suzana Hamdan − *Department of Biochemistry and Molecular Biology, University of Miami School of Medicine, Miami, Florida 33136, United States; Dr. JT Macdonald Foundation*

https://doi.org/10.1021/acsomega.1c05758
ACS Omega 2022, 7, 21359−21369

Biomedical Nanotechnology Institute of the University of Miami, Miami, Florida 33136, United States

Bapurao Surnar − *Department of Biochemistry and Molecular Biology, University of Miami School of Medicine, Miami, Florida 33136, United States; Dr. JT Macdonald Foundation Biomedical Nanotechnology Institute of the University of Miami, Miami, Florida 33136, United States; Sylvester Comprehensive Cancer Center, Miami, Florida 33136, United States;* orcid.org/0000-0001-5997-3120

Alexia L. Kafkoutsou − *Department of Biochemistry and Molecular Biology, University of Miami School of Medicine, Miami, Florida 33136, United States; Dr. JT Macdonald Foundation Biomedical Nanotechnology Institute of the University of Miami, Miami, Florida 33136, United States*

Luciano Magurno − *Department of Biochemistry and Molecular Biology, University of Miami School of Medicine, Miami, Florida 33136, United States*

Sapna K. Deo − *Department of Biochemistry and Molecular Biology, University of Miami School of Medicine, Miami, Florida 33136, United States; Dr. JT Macdonald Foundation Biomedical Nanotechnology Institute of the University of Miami, Miami, Florida 33136, United States; Sylvester Comprehensive Cancer Center, Miami, Florida 33136, United States;* orcid.org/0000-0002-4926-5355

Dushyantha T. Jayaweera − *University of Miami Clinical and Translational Science Institute, Miami, Florida 33136, United States; Department of Medicine, Miami Center for AIDS Research Leonard M. Miller, University of Miami School of Medicine, Miami, Florida 33136, United States*

Shanta Dhar − *Department of Biochemistry and Molecular Biology, University of Miami School of Medicine, Miami, Florida 33136, United States; Dr. JT Macdonald Foundation Biomedical Nanotechnology Institute of the University of Miami, Miami, Florida 33136, United States; Sylvester Comprehensive Cancer Center, Miami, Florida 33136, United States;* orcid.org/0000-0003-3042-5272

Complete contact information is available at: https://pubs.acs.org/10.1021/acsomega.1c05758

Notes

The authors declare no competing financial interest.

■ ACKNOWLEDGMENTS

S. Dhar, S. Daunert, S. Deo, and D.T. Jayaweera acknowledge the financial support from the Florida Department of Health Zika Research Grant Initiative award number 7ZK28. S. Daunert and S. Deo would like to acknowledge the financial support from the National Institute of Neurological Disorders and Stroke Grant award No. 1R21NS118427. S. Dhar thanks the Sylvester Comprehensive Cancer Center. S. Daunert is grateful to the Miller School of Medicine of the University of Miami for the Lucille P. Markey Chair in Biochemistry and Molecular Biology. We thank Dr. Mohammad Z. Kamran for his help with NS1 plasmid preparation and isolation. The authors are also grateful to Drs. Emre Dikici, Jean-Marc Zingg, and Yu-Ping Yang for their valuable assistance and guidance.

■ ABBREVIATIONS

Nano-IVM; nano-ivermectin; Caco-2 Cells; human epithelial colorectal adenocarcinoma cells; HEK293 cells; human embryonic kidney 293 cells; NS1 protein; nonstructural 1 protein; AST; aspartate aminotransferase; ALT; alanine aminotransferase.

■ REFERENCES

(1) Grimaldi, N.; Andrade, F.; Segovia, N.; Ferrer-Tasies, L.; Sala, S.; Veciana, J.; Ventosa, N. Lipid-Based Nanovesicles for Nanomedicine. *Chem. Soc. rev* **2016**, *45* (23), 6520−6545.

(2) Kasai, H.; Murakami, T.; Ikuta, Y.; Koseki, Y.; Baba, K.; Oikawa, H.; Nakanishi, H.; Okada, M.; Shoji, M.; Ueda, M.; Imahori, H.; Hashida, M. Creation of Pure Nanodrugs and Their Anticancer Properties. *Ang. Chem. Internat. Ed* **2012**, *51* (41), 10315−10318.

(3) Abdel-Hafez, S. M.; Hathout, R. M.; Sammour, O. A. Curcumin-Loaded Ultradeformable Nanovesicles as a Potential Delivery System for Breast Cancer Therapy. *Coll. and surf. B, Bioint* **2018**, *167*, 63−72.

(4) Goh, W. J.; Zou, S.; Ong, W. Y.; Torta, F.; Alexandra, A. F.; Schiffelers, R. M.; Storm, G.; Wang, J.-W.; Czarny, B.; Pastorin, G. Bioinspired Cell-Derived Nanovesicles versus Exosomes as Drug Delivery Systems: a Cost-Effective Alternative. *Sci. Rep* **2017**, *7* (1), 14322.

(5) Zhang, P.; Liu, G.; Chen, X. Nanobiotechnology: Cell membrane-Based Delivery Systems. *Nano Today* **2017**, *13*, 7−9.

(6) Hu, C.-M. J.; Zhang, L.; Aryal, S.; Cheung, C.; Fang, R. H.; Zhang, L. Erythrocyte Membrane-Camouflaged Polymeric Nanoparticles as a Biomimetic Delivery Platform. *Proc. Nat. Acad. Scien* **2011**, *108* (27), 10980−10985.

(7) Gao, W.; Zhang, L. Engineering Red-Blood-Cell-Membrane−Coated Nanoparticles for Broad Biomedical Applications. *AIChE J.* **2015**, *61* (3), 738−746.

(8) Vlassov, A. V.; Magdaleno, S.; Setterquist, R.; Conrad, R. Exosomes: Current Knowledge of Their Composition, Biological Functions, and Diagnostic and Therapeutic Potentials. *Biochim. Bioph. Acta (BBA) - Gen. Subj* **2012**, *1820* (7), 940−948.

(9) Uzoigwe, C. The Human Erythrocyte has Developed the Biconcave Disc Shape to Optimise the Flow Properties of the Blood in the Large Vessels. *Med. hypo* **2006**, *67* (5), 1159−1163.

(10) Rikken, R. S. M.; Engelkamp, H.; Nolte, R. J. M.; Maan, J. C.; van Hest, J. C. M.; Wilson, D. A.; Christianen, P. C. M. Shaping Polymersomes into Predictable Morphologies via out-of-Equilibrium Self-Assembly. *Nat. Commun.* **2016**, *7*, 12606.

(11) Srivastava, A.; Filant, J.; Moxley, K. M.; Sood, A.; McMeekin, S.; Ramesh, R. Exosomes: a Role for Naturally Occurring Nanovesicles in Cancer Growth, Diagnosis and Treatment. *Curr. gen. ther* **2015**, *15* (2), 182−192.

(12) Subbiah, N.; Campagna, J.; Spilman, P.; Alam, M. P.; Sharma, S.; Hokugo, A.; Nishimura, I.; John, V. Deformable Nanovesicles Synthesized through an Adaptable Microfluidic Platform for Enhanced Localized Transdermal Drug Delivery. *J. Drug Deliv* **2017**, *2017*, 1−12.

(13) Quan, L.; Liu, S.; Sun, T.; Guan, X.; Lin, W.; Xie, Z.; Huang, Y.; Wang, Y.; Jing, X. Near-Infrared Emitting Fluorescent BODIPY Nanovesicles for in Vivo Molecular Imaging and Drug Delivery. *ACS Appl. Mater. & Interf* **2014**, *6* (18), 16166−16173.

(14) Fais, S.; O'Driscoll, L.; Borras, F. E.; Buzas, E.; Camussi, G.; Cappello, F.; Carvalho, J.; Cordeiro da Silva, A.; Del Portillo, H.; El Andaloussi, S.; Ficko Trček, T.; Furlan, R.; Hendrix, A.; Gursel, I.; Kralj-Iglic, V.; Kaeffer, B.; Kosanovic, M.; Lekka, M. E.; Lipps, G.; Logozzi, M.; Marcilla, A.; Sammar, M.; Llorente, A.; Nazarenko, I.; Oliveira, C.; Pocsfalvi, G.; Rajendran, L.; Raposo, G.; Rohde, E.; Siljander, P.; van Niel, G.; Vasconcelos, M. H.; Yáñez-Mó, M.; Yliperttula, M. L.; Zarovni, N.; Zavec, A. B.; Giebel, B. Evidence-Based Clinical Use of Nanoscale Extracellular Vesicles in Nanomedicine. *ACS Nano* **2016**, *10* (4), 3886−3899.

(15) Wan, Y.; Wang, L.; Zhu, C.; Zheng, Q.; Wang, G.; Tong, J.; Fang, Y.; Xia, Y.; Cheng, G.; He, X.; Zheng, S.-Y. Aptamer-Conjugated Extracellular Nanovesicles for Targeted Drug Delivery. *Canc. Res.* **2018**, *78* (3), 798−808.

(16) Molinaro, R.; Evangelopoulos, M.; Hoffman, J. R.; Corbo, C.; Taraballi, F.; Martinez, J. O.; Hartman, K. A.; Cosco, D.; Costa, G.; Romeo, I.; Sherman, M.; Paolino, D.; Alcaro, S.; Tasciotti, E. Design

and Development of Biomimetic Nanovesicles Using a Microfluidic Approach. *Adv. Mater.* **2018**, *30* (15), 1702749.
(17) Laing, R.; Gillan, V.; Devaney, E. Ivermectin - Old Drug, New Tricks? *Tr. parasit* **2017**, *33* (6), 463−472.
(18) Barrows, N. J.; Campos, R. K.; Powell, S. T.; Prasanth, K. R.; Schott-Lerner, G.; Soto-Acosta, R.; Galarza-Munoz, G.; McGrath, E. L.; Urrabaz-Garza, R.; Gao, J.; Wu, P.; Menon, R.; Saade, G.; Fernandez-Salas, I.; Rossi, S. L.; Vasilakis, N.; Routh, A.; Bradrick, S. S.; Garcia-Blanco, M. A. A Screen of FDA-Approved Drugs for Inhibitors of Zika Virus Infection. *Cell host & microbe* **2016**, *20* (2), 259−270.
(19) Saiz, J.-C.; Martín-Acebes, M. A. The Race To Find Antivirals for Zika Virus. *Antimicrob. Agents Chemother.* **2017**, *61* (6), e00411−17.
(20) Caly, L.; Druce, J. D.; Catton, M. G.; Jans, D. A.; Wagstaff, K. M. The FDA-approved Drug Ivermectin inhibits the replication of SARS-CoV-2 in vitro. *Antivir. Res.* **2020**, *178*, 104787−104791.
(21) Surnar, B.; Kamran, M. Z.; Shah, A. S.; Basu, U.; Kolishetti, N.; Deo, S.; Jayaweera, D. T.; Daunert, S.; Dhar, S. Orally Administrable Therapeutic Synthetic Nanoparticle for Zika Virus. *ACS Nano* **2019**, *13* (10), 11034−11048.
(22) Lo, P.-K. A.; Williams, J. B. Solubilization of Ivermectin in Water. EP Patent EP0045655A2, 1983.
(23) Junyaprasert, V. B.; Morakul, B. Nanocrystals for Enhancement of Oral Bioavailability of Poorly Water-Soluble Drugs. *As. J. Pharm. Scien* **2015**, *10* (1), 13−23.
(24) Nakanishi, H. O. H. Reprecipitation Method for Organic Nanocrystals. In *Single Organic Nanoparticles*; Masuhara, H. N.; Sasaki, K., Eds.; Springer Berlin Heidelberg, 2003; pp 17−31.
(25) Hamdan, S.; Dumke, J. C.; El-Zahab, B.; Das, S.; Boldor, D.; Baker, G. A.; Warner, I. M. Strategies for Controlled Synthesis of Nanoparticles Derived from a Group of Uniform Materials Based on Organic Salts. *J. coll. interf. scien* **2015**, *446*, 163−169.
(26) Junnila, S.; Hanski, S.; Oakley, R. J.; Nummelin, S.; Ruokolainen, J.; Faul, C. F. J.; Ikkala, O. Effect of Double-Tailed Surfactant Architecture on the Conformation, Self-Assembly, and Processing in Polypeptide−Surfactant Complexes. *Biomacromolecules* **2009**, *10* (10), 2787−2794.
(27) Li, D.; Muller, M. B.; Gilje, S.; Kaner, R. B.; Wallace, G. G. Processable Aqueous Dispersions of Graphene Nanosheets. *Nat. Nanotechnol* **2008**, *3* (2), 101−105.
(28) Rolim, L. A.; dos Santos, F. C. M.; Chaves, L. L.; Goncalves, M. L. C. M.; Freitas-Neto, J. L.; da Silva do Nascimento, A. L.; Soares-Sobrinho, J. L.; de Albuquerque, M. M.; do Carmo Alves de Lima, M.; Rolim-Neto, P. J. Preformulation Study of Ivermectin Raw Material. *J. Therm. Anal. Calorim.* **2015**, *120* (1), 807−816.
(29) Gao, L.; Liu, G.; Ma, J.; Wang, X.; Zhou, L.; Li, X. Drug Nanocrystals: In Vivo Performances. *J. Contr. Release* **2012**, *160* (3), 418−430.
(30) Heurtault, B.; Saulnier, P.; Pech, B.; Proust, J.-E.; Benoit, J.-P. Physico-Chemical Stability of Colloidal Lipid Particles. *Biomaterials* **2003**, *24* (23), 4283−4300.
(31) Asahi, T.; Sugiyama, T.; Masuhara, H. Laser Fabrication and Spectroscopy of Organic Nanoparticles. *Acc. Chem. Res.* **2008**, *41* (12), 1790−1798.
(32) Fu, H.-B.; Yao, J.-N. Size Effects on the Optical Properties of Organic Nanoparticles. *J. Am. Chem. Soc.* **2001**, *123* (7), 1434−1439.
(33) De Montigny, P.; Shim, J.-S. K.; Pivnichny, J. V. Liquid Chromatographic Determination of Ivermectin in Animal Plasma with Trifluoroacetic Anhydride and N-Methylimidazole as the Derivatization Reagent. *J. Pharm. Biom. Anal* **1990**, *8* (6), 507−511.
(34) Vesterkvist, P. S. M.; Misiorek, J. O.; Spoof, L. E. M.; Toivola, D. M.; Meriluoto, J. A. O. Comparative Cellular Toxicity of Hydrophilic and Hydrophobic Microcystins on Caco-2 cells. *Toxins (Basel)* **2012**, *4* (11), 1008−1023.
(35) Róka, E.; Ujhelyi, Z.; Deli, M.; Bocsik, A.; Fenyvesi, É.; Szente, L.; Fenyvesi, F.; Vecsernyés, M.; Váradi, J.; Fehér, P.; Gesztelyi, R.; Félix, C.; Perret, F.; Bácskay, I. K. Evaluation of the Cytotoxicity of α-Cyclodextrin Derivatives on the Caco-2 Cell Line and Human Erythrocytes. *Molecules* **2015**, *20* (11), 20269−20285.
(36) Bailey, M. J.; Duehr, J.; Dulin, H.; Broecker, F.; Brown, J. A.; Arumemi, F. O.; Bermúdez González, M. C.; Leyva-Grado, V. H.; Evans, M. J.; Simon, V.; Lim, J. K.; Krammer, F.; Hai, R.; Palese, P.; Tan, G. S. Human Antibodies Targeting Zika Virus NS1 Provide Protection Against Disease in a Mouse Model. *Nat. Commun.* **2018**, *9* (1), 4560.
(37) Jia, L. Nanoparticle Formulation Increases Oral Bioavailability of Poorly Soluble Drugs: Approaches Experimental Evidences and Theory. *Curr. Nanosci* **2005**, *1* (3), 237−243.
(38) Shi, Y.; Porter, W.; Merdan, T.; Chiu, L. Recent Advances in Intravenous Delivery of Poorly Water-Soluble Compounds. *Expert Opinion on Drug Delivery* **2009**, *6* (12), 1261−1282.
(39) Onoue, S.; Yamada, S.; Chan, H.-K. Nanodrugs: Pharmacokinetics and Safety. *Int. J. Nanomedicine* **2014**, *9*, 1025−1037.
(40) Zamboni, W. C. Liposomal, Nanoparticle, and Conjugated Formulations of Anticancer Agents. *Clin. Canc. Res.* **2005**, *11* (23), 8230−8234.
(41) Yang, L.; Kuang, H.; Zhang, W.; Aguilar, Z.; Wei, H.; Xu, H. Comparisons of the Biodistribution and Toxicological Examinations after Repeated Intravenous Administration of Silver and Gold nanoparticles in Mice. *Sci. Rep* **2017**, *7*, 3303−3315.
(42) Barua, S.; Mitragotri, S. Challenges Associated with Penetration of Nanoparticles Across Cell and Tissue Barriers: A Review of Current Status and Future Prospects. *Nano today* **2014**, *9* (2), 223−243.
(43) Li, Z.; Xiao, C.; Yong, T.; Li, Z.; Gan, L.; Yang, X. Influence of Nanomedicine Mechanical Properties on Tumor Targeting Delivery. *Chem. Soc. Rev.* **2020**, *49* (8), 2273−2290.

https://doi.org/10.1021/acsomega.1c05758
ACS Omega 2022, 7, 21359−21369